Carbohydrate Polymers 92 (2013) 1348–1356

Contents lists available at SciVerse ScienceDirect

Carbohydrate Polymers

journal homepage: www.elsevier.com/locate/carbpol

Complexation of copper(II) with chitosan nanogels: Toward control of microbial growth

Fabrice Brunel, Nour Eddine El Gueddari, Bruno M. Moerschbacher*

IBBP, University of Münster, Schlossplatz 8, 48143 Münster, Germany

ARTICLE INFO

Article history:
Received 30 May 2012
Received in revised form 8 October 2012
Accepted 10 October 2012
Available online 17 October 2012

Keywords:
Adsorption
Chitin/chitosan
Antifungal activity
Nanoparticle, Hydrogel

ABSTRACT

Pure chitosan nanogels were produced, used to adsorb copper(II), and their antimicrobial activities were assessed. The complexation of copper(II) with chitosan solutions and dispersions was studied using UV–vis spectrometry. The adsorption capacity of chitosan nanogels was comparable to that of chitosan solutions, but copper(II)-loaded nanogels were more stable (i.e. no flocculation was observed while chitosan solutions showed macroscopic gelation at high copper concentration) and were easier to handle (i.e. no increase in viscosity). Adsorption isotherms of copper(II) onto chitosan were established and the impact of the pH on copper(II) release was investigated. The formation of a copper(II)–chitosan complex strongly depended on pH. Hence, release of copper(II) can be triggered by a decrease in pH (i.e. the protonation of chitosan amino groups). Furthermore, chitosan nanohydrogels were shown to be a suitable substrate for chitosan hydrolytic enzymes. Finally, a strong synergistic effect between chitosan and copper in inhibiting *Fusarium graminearum* growth was observed. The suitability of these copper(II)–chitosan colloids as a new generation of copper-based bio-pesticides, i.e. as a bio-compatible, bio-active and pH-sensitive delivery system, is discussed.

© 2012 Elsevier Ltd. All rights reserved.

1. Introduction

Infections by pathogenic microorganisms have been the cause of large scale famines and economic displacements in the past, and they are still responsible for significant losses to agricultural crops. A number of chemical agents exploiting different molecular modes of action have been developed for control of microbial infections of agricultural products. Ideally, the material should be of low toxicity to crops and to animals including humans, effective at low concentration on a wide range of microorganisms, stable during storage and use, but quickly and safely degraded in the environment, easy to employ, and preferably low in cost. Not surprisingly, no fully satisfactory chemical agents have been developed to date. Often, fungal control agents exhibit unwanted toxicity, so restrictions need to be placed on their use, or they are effective only against specific types of fungi, so that a number of separate agents must be employed to give comprehensive control. Also, an ever increasing number of fungal species have developed resistance against commonly employed fungicides.

Copper-based fungicides are key tools in disease prevention and treatment on a large variety of plants (Borkow & Gabbay, 2005). The mixture of copper sulfate and calcium hydroxide called "*Bouillie Bordelaise*" has been successfully used in vineyards since its first use in 1885 against downy mildew, an oomycete disease affecting a wide range of crop plants including grapes (Millardet, 1885). Copper-based fungicides are approved for organic farming, and they are still among the most effective agents for the control of many plant diseases. Applying copper might cause long-term contamination of the soil, whereas effects on water quality are estimated to be marginal. Copper compounds can build up in the soil and should not exceed the limits specified for heavy metals (Deluisa et al., 1996). Therefore, many copper compounds and complexes have been developed to improve the efficacy of copper-based products, concomitantly reducing the amount of copper required to achieve disease control (Benns, Gingras, & Bayley, 1960; Ivanov, Tikhomirova, Tomchin, & Razukrantova, 1989; Johna, Sreekantha, Rajakannanb, Ajithc, & Prathapachandra Kurup, 2004).

Chitosans, a family of linear and partly acetylated (1-4)-2-amino-2-deoxy-β-D-glucans (Hoppe-Seiler, 1894; Moerschbacher, Bernard, & El Gueddari, 2011; Muzzarelli, 1977, 2012; Rouget, 1859), are natural polysaccharides obtained commercially by deacetylation of chitin extracted e.g. from shrimps or crab shells (Lamarque, Viton, & Domard, 2004a, 2004b). There are several reasons why chitosans may be used as an effective formulation for copper as a plant protectant. Firstly, the ability of chitosans to form complexes with transition metal ions is well known (Chiessi, Paradossi, Venanzi, & Pispisa, 1992; Domard, 1987; Monteiro & Airoldi, 1999; Rhazi et al., 2002), so that chitosan–copper

* Corresponding author. Tel.: +49 251 8324794; fax: +49 251 8328371.
E-mail address: moersch@uni-muenster.de (B.M. Moerschbacher).

0144-8617/$ – see front matter © 2012 Elsevier Ltd. All rights reserved.
http://dx.doi.org/10.1016/j.carbpol.2012.10.025

complexes may serve as a reservoir for the slow release of antimicrobially active copper(II) ions. Concomitantly, partially acetylated chitosans may act as a sticker immobilizing copper on the hydrophobic leaf surface. Secondly, chitosans have demonstrated antimicrobial activity against a wide range of bacteria and fungi, with potential applications in crop protection (Kong, Chen, Xing, & Park, 2010; Oliveira, El Gueddari, Moerschbacher, Peter, & Franco, 2008). Thirdly, chitosans are known to act as a plant growth promoters (Luan et al., 2005). The exact mechanism by which chitosans exert their bio-activities is unknown; however, factors that can influence bio-activities include the average molecular weight or degree of polymerization (DP) and the degree of acetylation (DA) of the chitosan used, and the pH of the test medium (Oliveira et al., 2008).

Antimicrobial activities of chitosans are usually reported using the soluble form of chitosan (Rabea, Badawy, Stevens, Smagghe, & Steurbaut, 2003), while chitosan complexes with transition metals are mainly obtained with an insoluble form of chitosan, namely cross-linked chitosan, or with chitosan derivatives (Chiessi et al., 1992; Varma, Deshpande, & Kennedy, 2004). The elaboration of chitosan particles loaded with copper has been reported as potential waste water treatment (Wan Ngah, Endud, & Mayanar, 2002; Wu, Liou, Yeh, Mi, & Lin, 2012; Yan et al., 2012) or anticancer chemotherapeutic agent (Qi, Xu, Jiang, Li, & Wang, 2005; Zheng et al., 2006). In this work, we propose to investigate the use of chitosan particles loaded with copper as an antimicrobial agent. Recently, a new process to elaborate pure chitosan nanogels has been developed using physical gelation in reverse emulsion (Brunel, Veron, David, Domard, & Delair, 2008). These chitosan nanogels could perfectly fulfill the requirements for the development of an effective and fully bio-compatible plant protectant: the core of the nanogels containing neutralized amino groups could provide efficient correlation complex of copper while the charged amino groups on the surface could still ensure the stability of the dispersed material in water and so facilitate handling (Brunel et al., 2009).

2. Materials and methods

2.1. Materials

The oil phase used to prepare the water-in-oil emulsion was composed of medium-chain triglycerides from capric/caprilic acid (Miglyol 812N, Sasol®, Germany) and a surfactant, sorbitan monooleate (Span 80, Fluka®, Germany). Chitosan, obtained from squid pens, was provided by Mahtani Chitosan PVT. LTD. India (DA ca. 5%, weight–average molar mass M_w = 400,000 ± 20,000 g mol^{-1} i.e. DP ca. 2000). Copper acetate was purchased from Fluka. Chitosan N-acetylglucosaminohydrolase from *Streptomyces* sp. (chitosanase) was purchased from Sigma–Aldrich (Germany). A strain of *Fusarium graminearum* (Schwabe) isolated in Wuhan (China) was used. It was kindly provided by Dr. Yu-Cai Liao (Institut für Biologie II, RWTH Aachen, Germany).

2.1.1. Chitosan preparation

2.1.1.1. Purification. Prior to use, the polymer was purified as follows: dissolution in a 0.1 M acetic acid solution, filtration through Millipore membranes of decreasing porosity (from 3 to 0.22 μm), precipitation with ammonia, rinsing with de-ionized water until neutrality, and freeze-drying.

2.1.1.2. Depolymerization. A nitrous de-amination/depolymerization using sodium nitrite was carried out according to Allan & Peron to produce low molar mass polymers (Allan & Peyron, 1995a, 1995b). Low molar mass chitosans were recovered by precipitation with ammonia, then purified by several washings with de-ionized water until neutrality, and finally lyophilized. The final molar mass of chitosan was M_w = 11,000 ± 1000 g mol^{-1}, i.e. DP ca. 50, and I_p = 1.7, determined as described in Section 2.1.2.1.

2.1.1.3. Acetylation. This low molar mass chitosan was partially re-N-acetylated using acetic anhydride in homogeneous medium to reach DA 10%. The reaction was performed in a hydro-alcoholic mixture according to the procedure previously described by Vachoud, Zydowicz, and Domard (1997). After re-acetylation, chitosans were neutralized, rinsed with de-ionized water, and freeze-dried. The degree of acetylation (DA) of the final chitosan was determined using ^{1}H NMR spectroscopy (Varian, 500 MHz), according to the method developed by Hirai, Odani, and Nakajima (1991).

2.1.2. Chitosan characterization

2.1.2.1. Size exclusion chromatography. The weight-average molecular weight (M_w) and the polydispersity index (I_p) were measured by gel permeation chromatography on a HP-SEC system (Polymer Standards Service GmbH, Germany) consisting of Novema columns 100 Å, 3000 Å, and guard column (I.D. 8 mm) (PSS) coupled online with a refractive index detector (Agilent series 1200 RID), a UV detector (Agilent 1200 Series Variable Wavelength Detector), a viscometer detector (PSS ETA-2010 differential viscometer) and multi-angle-laser-light-scattering (PSS SLD 7000 MALLS) equipped with a 5 mW He/Ne laser operating at λ = 632.8 nm. Light intensity measurements were derived following the classical Rayleigh–Debye equation allowing to deduce M_w (WinGPC UNITY). A degassed 0.2 M acetic acid/0.15 M ammonium acetate buffer (pH = 4.5) was used as an eluent. For accurate concentration measurements, the refractive index increments (dn/dc) were determined independently for each sample using a differential refractometer (BI-DNDCW, Brookhaven Instruments Corporation, NYC, USA) in the same solvent, operating at λ = 632.8 nm.

2.1.2.2. Thin layer chromatography. Chitosan oligomers were analyzed using HP-TLC. Briefly, 10 μL of the supernatant were applied on Silica Gel 60F$_{254}$ plates (Sigma–Aldrich, Germany) with an Automatic TLC Sampler 4 piloted by the Wincats software 1.3.2 (Camag, Switzerland). A mixture of butanol (41.7%), methanol (33.3%), ammonium solution 25% (16.7%), and water (8.3%) was used as an eluent, oligomers were stained using a mixture of acetone (4 mL), diphenylamine (80 mg), aniline (80 μL), and orthophosphoric acid 85% (600 μL), and heated at 150 °C for about 10 min.

2.1.3. Chitosan nanogel synthesis

Nanohydrogels were prepared by physical gelation in reverse emulsion. Aqueous chitosan solution (10 mL, 20 mg mL^{-1} chitosan) was emulsified in 40 mL of Miglyol 812N containing 0.5 g Span 80 with a sonotrode (Bandelin KE76, Berlin, Germany). A stream of ammonia increased the pH of the medium up to 9 which triggered the gelation of the chitosan droplets. Finally, the dispersion was centrifuged at 1000 × g for 15 min, washed twice with ethanol and twice with water, then redispersed in an ammonium acetate buffer (50 mM at pH 4.5) by slow stirring overnight (Brunel et al., 2008).

2.1.4. Chitosan nanogel characterization

2.1.4.1. Photon correlation spectroscpoy. The size and size distribution of the nanogels were determined at 173° with a Zetasizer NanoZS (Malvern Instruments Ltd., Worcestershire, UK) equipped with a 4 mW He/Ne laser beam operating at λ = 633 nm. All measurements were performed at 25.0 ± 0.2 °C. The self-correlation function was expanded in a power series (Cumulants methods) (Koppel, 1972). The polydispersity value provided by the software is a dimensionless parameter PDI defined as the ratio $\mu_2/(\Gamma)^2$, where μ_2 is the second cumulant of the correlation function and (Γ) the average decay rate. Each value was the average of three

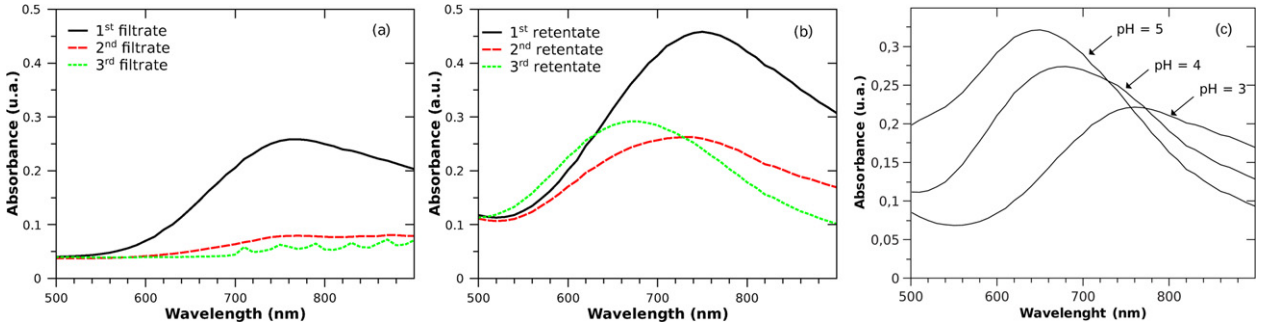

Fig. 1. Absorbance spectrum of free (a) and chitosan-bound (b) copper(II) recovered by ultrafiltration in the filtrate and the retentate, respectively, during the washing steps of copper-loaded chitosan nanoparticles and (c) copper(II)-loaded chitosan nanogels after washing and mixing with the same volume of 50 mM ammonium acetate buffer at different pH values.

series of ten measurements. The pH of the suspension was varied by addition of small amounts of aqueous ammonia or acetic acid. Zeta potentials were derived, using Smoluchowski's equation, from electrophoretic mobility measurements obtained from the same instrument (Smoluchowski, 1903).

2.1.4.2. Transmission electron microscopy. Micrographies of the particles were obtained using a Zeiss EM900 electron microscope operating at 80 kV with a resolution of 0.5 nm and a magnification range of 150–250,000×. A droplet of particle suspension in ammonium acetate buffer (50 mM at pH 4.5) with a solid content of 0.3% (w/v) was deposited during one minute on a silver specimen grid. Once the particles were adsorbed onto the film surface, excess sample was blotted off and the grid covered with a small drop (5 μL) of staining solution (1%, w/w solution of uranyl acetate at pH 4.5). The latter was left on the grid for a few minutes and then blotted off. The sample was then dried and examined by TEM.

2.1.5. Copper loading

Copper acetate solutions (250 μL) of different concentrations were mixed overnight at room temperature with the chitosan nanogel suspension in a 50 mM ammonium acetate/acetic acid solution. Adsorption isotherms were first established at pH 4.5, then the effect of the pH was studied by adding small amounts of acetic acid or ammonia. After incubation with the nanogels, the free copper(II) was recovered by ultrafiltration using Vivaspin devices (PES membrane with a MWCO of 10,000 Da, then centrifuged at 10,000 × *g* for 10 min). The loaded nanogels were washed three times with water using the same ultrafiltration method. The concentration of free copper(II) ions in the filtrate was assayed by measuring the absorbance at 750 nm, i.e. the red region of the spectrum (responsible for the blue color of copper(II) aqueous solutions). Absorbance values were recorded using a Spectramax M2 spectrophotometer (Molecular Devices, USA).

FT-IR spectra (spectral region 4000–400 cm^{-1}) were recorded on a Nicolet iS10 FT-IR Spectrometer (Thermo Fisher Scientific Inc.©). Prior to the measurement, chitosan, chitosan particles, and chitosan particles loaded with copper(II) were washed with water (as described above) and freeze dried. A few milligrams of the resulting powder was then mixed with 0.15 g KBr and pressed (10 bar for 30 s) to obtain a solid tablet. Pure KBr tablet was used as background.

2.1.6. Antifungal test

Complete medium (CM), pH 4.3, was prepared as described by Pontecorvo, Roper, Chemmons, Macdonald, and Bufton (1953). Aliquots (150 μL) of sterile CM containing the required volume of chitosan and copper (to give final concentrations ranging from 0 to 1 mg mL^{-1}) for the analysis of dose/response relationships and sterile water were dispensed into wells of 96-well polystyrene microtiter plates (Roth, Germany) containing either 10 μL of a spore suspension of a test fungus (*F. graminearum*) or 10 μL of sterile water (blanks). The plates were incubated at 25 °C under agitation, 200 opm (orbits per minute), for one week. Fungal growth was assessed by measuring the optical density of the culture media at 405 nm at 24 h intervals. Three independent experiments were carried out in triplicates each, and the data are reported as means ± SD. A standard curve was previously prepared to evaluate the correlation of absorbance values with dry weight of biomass. This calibration curve was found to be linear for the range between 0 and 4.0 for the fungus studied. According to Langvad, the absorbance at 405 nm is caused by light absorbance and light scattering (Langvad, 1999).

3. Results and discussion

3.1. Copper loading on chitosan nanogels

3.1.1. Copper(II) complex characterization

Prior to quantitatively investigating the absorption of copper(II) by chitosan particles, qualitative analyses of the octahedral copper(II) coordination complex were performed. Copper acetate was incubated with chitosan nanogels, free copper(II) and loaded nanogels were recovered in the filtrate and retentate of ultrafiltration, respectively. The suspension of nanogels bound with copper(II) was washed three times with water. Fig. 1 shows the absorption spectrum of the filtrate (Fig. 1a) and the retentate (Fig. 1b) after each washing step.

In aqueous solution, copper(II) ions showed an absorption maximum at 750 nm corresponding to the excitation of an electron of the d-orbital of copper from the t_{2g} level to the e_g level; the difference in energy between the d-orbitals is called splitting parameter (Musinu, Paschina, Piccaluga, & Magini, 1983), Δ_o. The absorbance of the filtrate, corresponding to the unbound copper(II), decreased rapidly during the washing process. After three washing steps, no copper(II) could be detected in the filtrate, hence to the detection limit of the spectrophotometer, it could be concluded that all free copper(II) had been washed out. Fig. 1b displays the same decrease of the absorbance at 750 nm in the retentate, but also a shift of the maximum absorbance upon the removal of free copper. Indeed, the magnitude of this energy difference in a transition metal complex depends on the nature of the ligand (Hathaway & Hodgson, 1973). After complexation with chitosan, the maximum absorbance of the copper(II) is shifting to a lower wavelength. Indeed, on the spectrochemical series, the ammonium ion is a stronger field ligand compared to water, resulting in a larger splitting parameter, Δ_o.

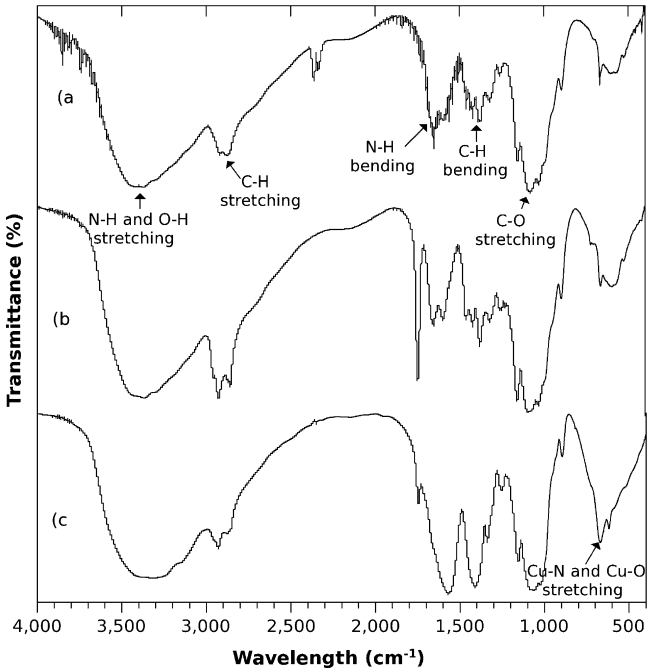

Fig. 2. FT-IR spectra of (a) chitosan, (b) chitosan particles, and (c) chitosan particles loaded with copper (II).

Therefore, the energy of the absorbed light is higher (i.e. lower wavelength). After three washing steps, no free copper remained in either the filtrate or the retentate, confirming the efficiency of the washing process. Importantly, the retentate containing the nanogels still retained copper(II) bound as a correlation complex with the chitosan. No impact of the pH (from 3.5 to 6) or of the buffer concentration (from 0 to 50 mM) on the absorption spectrum of free copper(II) were observed (data not shown). Therefore, the absorption at 750 nm of the first filtrate could be used to calculate the adsorption capacity of the chitosan, as the copper(II) concentration in the filtrate corresponds to the concentration of residual copper(II) in equilibrium with adsorbed copper(II). The copper detected in the further washing steps corresponds to the dilution of the free copper still present in the first retentate.

The presence of a chitosan–copper(II) correlation complex was confirmed using FT-IR spectrometry in the wavelength region between 4000 and 400 cm^{-1} (cf. Fig. 2). The frequencies of the IR absorption bands of chitosan and of the chitosan particles (Fig. 2a and b, respectively) were consistent with the assignments for chitosan. According to literature, powder chitosan exhibited a broad peak at 3450 cm^{-1}, which is assigned to the N—H and hydrogen bonded O—H stretch vibrational frequencies. The two peaks at 2880 cm^{-1} and 2920 cm^{-1} are assigned to the symmetric and asymmetric modes of CH_2 group vibrations, respectively. In addition, the characteristic band due to CH_2 scissoring, which occurs at 1420 cm^{-1}, was also present in the sample. The peaks at 1590 and 1650 cm^{-1} were assigned to N—H bending vibrations (N—H) of the secondary amide. The band which appears at 1075 cm^{-1} corresponds to the stretching of C—O bond of C3 (secondary OH). The band at 1025 cm^{-1} is produced by the C—O stretching of C6 of chitosan (primary OH). The asymmetric stretching of C—O—C appears at 1150 cm^{-1} (Lee, Mi, Shen, & Shyu, 2001; Osman & Arof, 2003).

The spectrum of chitosan nanoparticles loaded with copper(II) (Fig. 2c) showed significant differences compared to chitosan and chitosan nanoparticle spectra. First, the peaks due to the N—H bending vibrations at 1650 and 1590 cm^{-1} were overlapping and shifted toward lower frequency (1550 cm^{-1}), indicating the involvement of the amino groups in the complex formation (Mekahlia & Bouzid, 2009). Second, the modification of the shape and intensity of the C—H stretching and bending bands at 1420 cm^{-1} probably results from a modification in the environment of CH_2OH due to the presence of copper(II) intercalate in the crystal structure of chitosan. Finally, in the region between 3000 and 3700 cm^{-1}, N—H and hydrogen bonded O—H stretch vibrational frequencies exhibited a broader peak, due to a decrease in hydrogen bonding (Qi et al., 2005). Indeed, chitosan crystalline structure presents several hydrogen bonds which can be disrupted by the presence of a chitosan/metal complex (i.e. a larger unit cell) (Ogawa, Oka, & Yui, 1993). Therefore, the discrepancies observed when copper is added are very likely due to complexation of copper(II) with chitosan amino and hydroxyl groups as demonstrated by Monteiro and Airoldi (1999). Finally, it is worth noting that all spectra were recorded using freeze-dried samples, implying that the chitosan–copper(II) correlation complex remains stable after solvent evaporation.

The colloidal stability of the copper(II)–chitosan complexes was confirmed using Photon Correlation Spectroscopy and TEM. The size, polydispersity, and zeta potential of the nanogels remained constant after loading with copper(II) at 220 ± 10 nm, 0.2 ± 0.02, and $+40 \pm 3$ mV, respectively. The copper(II) loaded did not provide enough contrast for a direct observation in transmission electron microscopy; therefore, uranyl acetate staining was used. The stain precipitated onto the formavar grid after deposition of the particles. Thus, the particles appeared white on a dark background (negative staining). TEM experiments were reproduced with nanogels before (Fig. 4a) and after (Fig. 4b) copper loading, all the observed particles showed the same characteristics (with diameters ranging from 100 to 500 nm, similar polydispersity, spherical shapes), and no significant aggregation was observed. The background on the copper(II)–chitosan nanogel micrographs appears darker; this might be due to the presence of copper which diminished the contrast between the nanogels and the stain precipitate, but an artifact from the techniques cannot be excluded. The colloidal stability of the nanogels remained identical, thus the copper is probably loaded inside the nanogel (i.e. no impact of the bound copper(II) on the surface forces). This location of copper(II) was confirmed when the interaction between copper(II) and chitosan amino groups was investigated as a function of pH (see Section 3.1.3).

3.1.2. Adsorption isotherms

The copper adsorption isotherm on chitosan nanogels was compared to the copper complexation of soluble chitosan (Fig. 3a). The molar mass cutoff of the filter was about 10,000 Da; therefore, high molar mass chitosan (M_w = 450,000 $gmol^{-1}$) of the same DA as used for the preparation of the nanogels was used to separate the chitosan–copper(II) correlation complex from the free copper(II) ions. Gelation of high molar mass chitosan was observed for copper concentrations above 1.5 mg mL^{-1}; these copper–chitosan gels were spun down before filtration of the supernatant. The adsorption isotherm of copper with chitosan, as solution or dispersion, fit the Langmuir model (Langmuir, 1918). The Equation of a Langmuir type isotherm is given below, where C is the equilibrium solution concentration, Γ is the amount adsorbed in mg of copper per g of chitosan, Γ_{max} is the maximum amount adsorbed and K is the Langmuir equilibrium constant.

$$\Gamma = \frac{\Gamma_{max} \times K \times C}{1 + K \times C}$$

The Langmuir equilibrium constant K and the maximum amount adsorbed Γ_{max} describe the affinity of the substrate for this surface and the saturation of the surface, respectively. The calculated Langmuir equilibrium constants for chitosan solution and dispersion were 0.41 and 0.38 mL mg^{-1}, respectively, confirming the existence

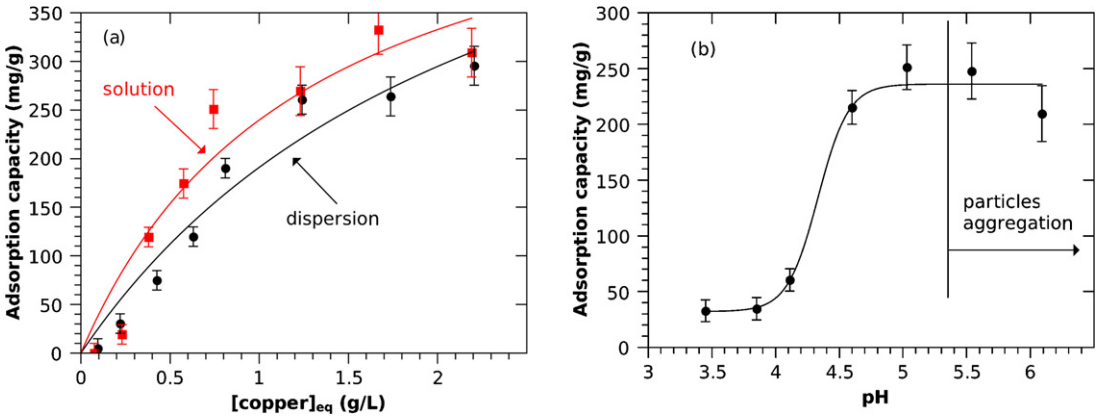

Fig. 3. (a) Adsorption isotherms of chitosan in solution and as a nano-dispersion (1 mg mL^{-1}) in 25 mM ammonium acetate buffer at pH 4.5. Data are average values from three independent experiments with Langmuir fit. (b) Adsorption capacity of chitosan nanogels (1 mg mL^{-1}) as a function of pH in 25 mM ammonium acetate buffer at pH 4.5. Data are average values from three independent experiments with a sigmoidal fit.

of a strong affinity between copper(II) ions and chitosan, through a correlation complex as demonstrated in Section 3.1.1.

The saturation of the nanogels is achieved with 1.5 mg mL^{-1} copper(II), with a maximum adsorption capacity of about 300 mg g^{-1}, suggesting that about 80% of the amino groups are complexed with one copper(II) ion each.

3.1.3. Effect of pH

Next, we analyzed the impact of pH on the absorption capacity (Fig. 3b) which is of critical importance as the amount of neutralized amine functions available for complexation increases with the pH, as shown by the evolution of the zeta potential of the particles as a function of pH (Brunel et al., 2009). For pH values close to neutrality (pH 5.5 to 6), the structure of the chitosan–copper(II) complex changes from type I {$[(Cu(-NH_2)]^{2+}$, $2OH^-$, H_2O)} to type II {$[(Cu(-NH_2)_2]^{2+}$, $2OH^-$)} as shown in Scheme 1 (Chiessi et al., 1992). When the second type of complex occurs, one further amino group is incorporated into the first complex which could lead to the binding of two chitosan chains from different particles (Rhazi et al., 2002). For pH values higher than the pK_a of chitosan (6.2) the deprotonation of the amino groups induces a decrease of the surface charge and the collapse of the interfacial chitosan, hence the drastic aggregation of the colloid observed.

The amount of copper(II) loaded in the chitosan nanogels strongly depended on the ionization degree of chitosan, which varies with pH. The maximum adsorption capacity was obtained at pH 5.5, while at lower pH, the complexation of copper with chitosan sharply decreased.

Interestingly, most fungi are acidophilic and tend to reduce the pH of their surrounding environment. The ability of *Fusarium* to acidify the extracellular pH has been demonstrated (Prusky & Yakoby, 2003), and can be due to the production of fusaric acid (Bacon, Portyer, Noreed, & Leslie, 1996) and oxalic acid (Swain & Ray, 2009). Thus, the acidification caused by the growth of a pathogen could unbind the copper(II). Therefore, the UV–vis spectra of copper(II)-loaded nanoparticles at different pH, after addition of a small amount of acetic acid, are presented in Fig. 1c. The decrease in pH triggered a shift of the maximum absorbance to a higher wavelength indicating the release of bound copper(II) due to protonation of the amino groups of chitosan as shown in Scheme 1. The intensity of the absorbance also decreased with pH, as the amino group is a stronger field ligand compared to water resulting in a more stable complex.

Finally, the absorbance at a wavelength lower than 550 nm also decreased with pH. This might result from the decrease in turbidity of the samples due to the better hydration and possible resolubilization of the chitosan nanogels in acidic media.

3.2. Bioactivty of copper(II)–chitosan complex

To predict the behavior of the copper(II)-loaded nanogel when used as a bio-pesticide, the impact of chitosanolytic enzymes on the particles and their antifungal activity against *F. graminearum* were investigated.

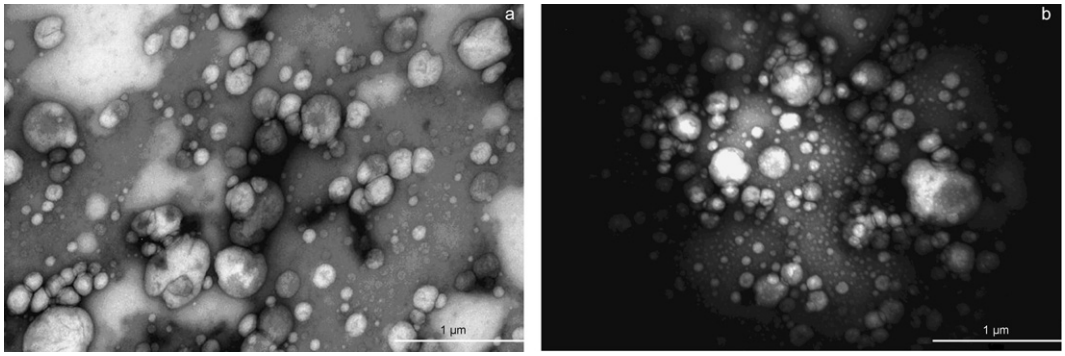

Fig. 4. Transmission electron micrographs of chitosan nanoparticles in the dry state, before (a) and after (b) copper(II) loading. Uranyl acetate (1% (w/w) in water, pH 4.5) was used as a negative stain.

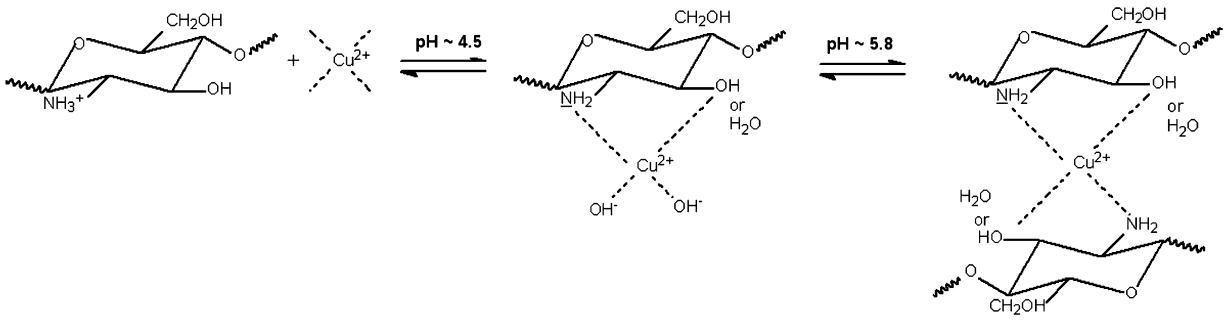

Scheme 1. Proposed mechanisms of the copper(II)–chitosan correlation complexes.

3.2.1. Enzymatic digestion

The enzymatic hydrolysis of chitosan in solution and as a dispersion, in the form of nanogels, was investigated using HP-SEC and QELS, respectively. A chitosan solution in ammonium acetate buffer (50 mM, pH 4.5) was incubated with chitosanase at room temperature in a HP-SEC vial, and an aliquot was injected onto the SEC-columns every hour. The weight average molar mass of the substrate was determined from the signal of the refractive index detector for all injections (Fig. 5a). The molar mass of chitosan decreased rapidly during the first hours of reaction, overnight incubation yielded small oligomers (DP < 10). Chitosan nanogel dispersions were incubated similarly, with chitosanase and the same buffer, in a cuvette, and analyzed by QELS every 5 min. The size, polydispersity (PDI), and mean count rate were recorded (Fig. 5b and c). During the first hours, the mean count rate and the PDI remained more or less constant while the average size of the particles slightly decreased. The reduction of the particle size might result from the activity of the enzyme. After a few hours, the mean count rate started decreasing rapidly, corresponding to a decline of the scattering intensity of the sample. The scattering intensity depends on the size and the number of particles, both could decrease due to the further degradation of the chitosan nanogels. Concomitantly, the average size of the particles increased as the smaller particles were the first to disappear; only the largest particles remained but became rapidly too dilute for an accurate measurement of their size, hence the high PDI. Thus, chitosan nanogels appear to be a suitable substrate for chitosanolytic enzymes. In order to confirm this result, the final products of the hydrolysis were further analyzed using HP-SEC and HP-TLC (Fig. 6). Chitosanase-treated and control nanogel samples were re-dissolved by the addition of acetic acid and injected into HP-SEC (Fig. 6 a). The elugram shows the presence of low molar mass chitosan (M_w = 11,000 g mol^{-1}) for the pure nanogels; this peak disappears upon enzymatic treatment and the generation

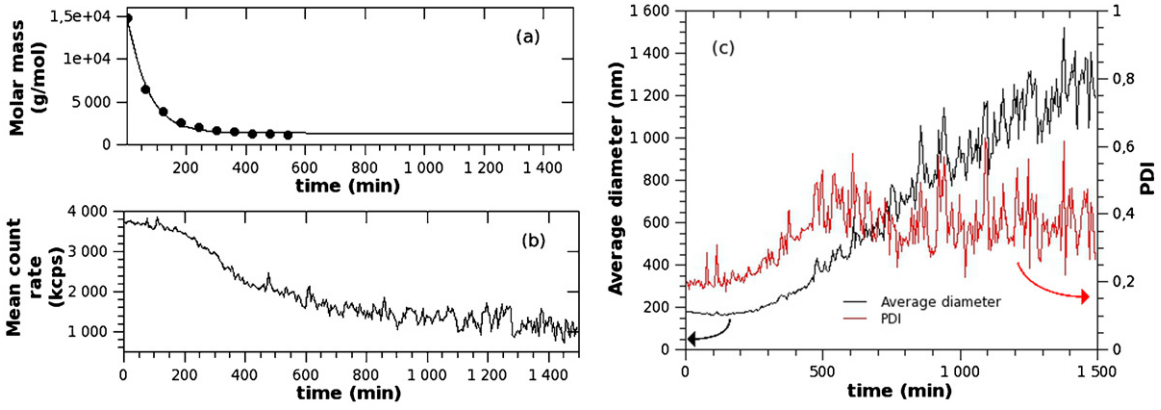

Fig. 5. Kinetics of hydrolysis of chitosan in solution and as a dispersion using chitosanase. The weight average molar mass of chitosan in solution (a) was measured using HP-SEC. The mean count rate (b), the average diameter and the PDI (c) of the particles were measured using QELS.

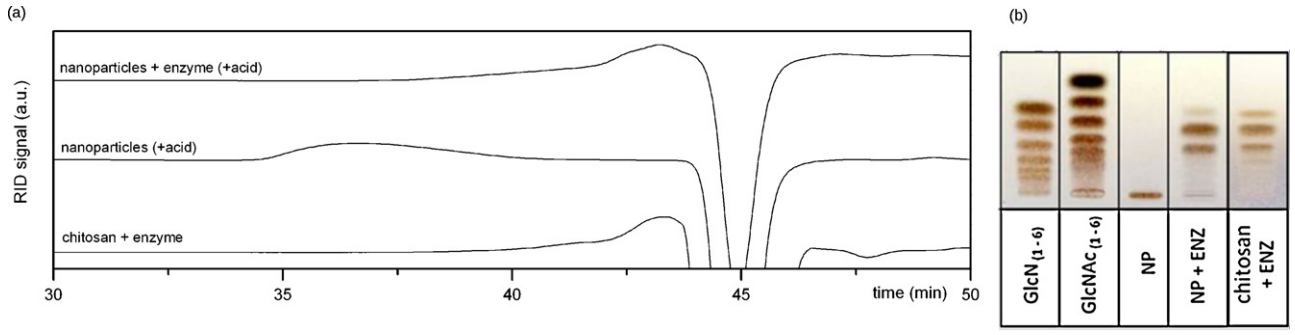

Fig. 6. HP-SEC analysis of re-dissolved chitosan nanogels before and after incubation with chitosanase, and HP-TLC analysis of the chitosan oligomers.

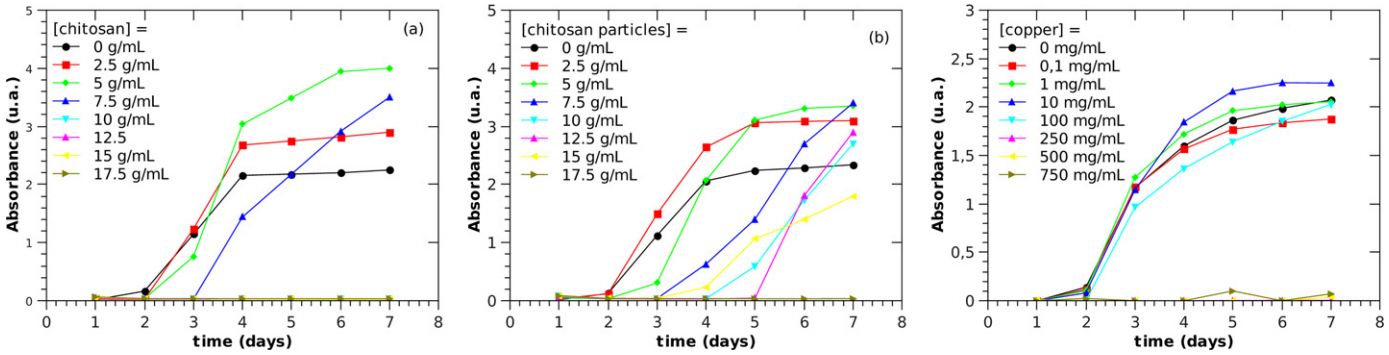

Fig. 7. Fungal growth in the presence of chitosan solutions, chitosan nanogels, and copper(II) at different concentrations.

of oligomers results in the appearance of a later peak at an elution time of ca. 43 min (close to the negative peak of the solvent at 45 min). Chitosan oligomers produced by enzymatic hydrolysis of chitosan in solution or in the form of nanogels were further characterized by HP-TLC; both consisted mainly of deacetylated glucosamine dimers and trimers, with some monomer and traces of larger oligomers. These results support the previous conclusion that chitosan nanogels are a suitable substrate for a chitosan hydrolase.

3.2.2. *Antifungal activity of copper-nanogels*

Growth rates of the fungus *F. graminearum* were determined in the presence of different concentrations of chitosan in solution or in the form of nanoparticles, or in the presence of copper(II) ions derived from copper acetate salt (Fig. 7). The minimum inhibitory concentration (MIC) of a compound was defined as the lowest concentration that will fully prevent visible growth of the microorganism after one week of incubation. The MIC of copper(II), chitosan solution, and chitosan nano-dispersions were determined as 250 $\mu g\,mL^{-1}$, 10 $mg\,mL^{-1}$, and 17.5 $mg\,mL^{-1}$, respectively. The chitosan nanogels were almost as active as the chitosan solution even though only part of the polymer, on the surface of the particles, is available for interacting with the fungal cell walls. A slight increase in growth rates at low chitosan concentrations is most likely due to the production and secretion of chitosanolytic enzymes by the fungus, allowing it to use chitosan as a C- and N-source (Oliveira et al., 2008).

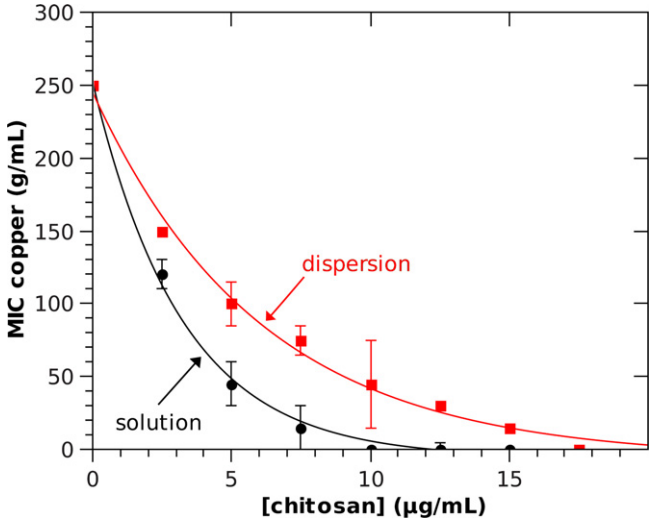

Fig. 8. Evolution of the MIC of copper(II) as a function of the concentration of chitosan (in solution or as a dispersion). Data are average values from three independent experiments with an exponential fit.

Then, the MIC of copper was determined in the presence of various concentrations of chitosan as a solution or nano-dispersion (Fig. 8). The MIC of copper(II) decreased exponentially when adding low amounts of chitosan either in solution or dispersion. Thus, copper(II) and chitosan are not only bio-compatible and bio-active, they also exhibit a strong synergistic effect in terms of their antifungal activities. As an example, the MIC of copper(II) was reduced from 250 to 75 or 15 $\mu g\,mL^{-1}$ in the presence of 7.5 $\mu g\,mL^{-1}$ of chitosan in dispersion or solution, respectively, i.e. by a factor of ca. 3 or 17, even though chitosan alone had no inhibitory activity at this low concentration. This synergistic effect is difficult to explain because the mechanism of the antifungal activities of chitosan is not well understood. Kong et al. (2010) located the chitosan on the plasma membrane and showed that chitosan induces leakage from lipid vesicles containing various compositions of fungal lipids. Copper toxicity has been largely attributed to its redox-properties. It can catalyze the production of highly reactive hydroxyl radicals which can subsequently damage lipids, proteins, DNA, and other biomolecules (Borkow & Gabbay, 2005). Therefore, it is possible that small amounts of chitosan and copper can cause significant disruption in membrane integrity, enabling more copper to get through the fungal membrane causing extensive damage within the cell. Hence, a very promising strategy for the growth control of microorganisms can be envisioned based on these results. Furthermore, the antifungal activity of chitosan nanoparticles is similar to that of chitosan in solution, although only a small fraction of the chitosan, which is present at the surface, can interact with the fungus. The use of chitosan dispersions can provide many advantages compared to a solution: lower viscosity, easier handling, good distribution on the leaves, and long-term release of copper on the leaves or in the soil with no loss of antifungal properties.

4. Conclusion

Pure chitosan nanogels were produced in relatively large amounts with a high yield, and loaded with copper(II). The adsorption capacity of this colloidal chitosan was comparable to that of chitosan in solution and strongly depended on pH. The maximum adsorption capacity for copper(II) was obtained at pH 5 where 300 mg of copper(II) were bound to 1 g of chitosan; under these conditions, 80% of the amino groups were complexed with a copper(II) ion.

These nanogels perfectly fulfill the requirement of a copper-based pesticide:

- First, the physico-chemical structure of the gel, composed of neutralized amino groups, is able to complex large amounts of copper(II).

- Second, the loading capacity strongly decreases in acid conditions, via the protonation of the amino groups; therefore, the acidification as caused by a growing pathogen, can unbind the loaded copper(II).
- In addition, the chitosan nanogels were shown to be a suitable substrate for chitosanolytic enzymes present in many phytopathogenic fungi (Oliveira et al., 2008), leading to the complete discharge of the copper(II) and the production of chitosan oligomers with potential plant strengthening activities.
- Finally, a synergistic effect of the chitosan and copper was observed in their antimicrobial effect against the phytopathogenic fungus *F. graminearum*.

The mode of action of copper(II) and chitosan as antimicrobial agents is not fully understood yet, and further studies using fluorescent chitosans are ongoing. However, chitosan nanogels can enhance the combined antimicrobial activity of both compounds and could be developed into an efficient delivery system for copper-based fungicides. A colloidal system also avoids problems brought about by the viscosity of chitosan solutions, ensuring easy handling and good distribution on the leaves, simultaneously conveying long term colloidal stability for storage. Hence, nano-colloidal chitosan particles are a promising, biocompatible and bioactive adjuvant for copper-based plant protectants, and they are currently being tested in vivo.

Role of the funding source

BMBF was not involved in study design; in the collection, analysis, and interpretation of data; in the writing of the report; or in the decision to submit the paper for publication.

Acknowledgements

We thank Frank Bernard and Ursula Fassin for their help with the chitosanolytic enzyme and *F. graminearum*, Dr. Dominique Gillet from Mahtani Chitosan for supplying the chitosan raw material, Dr. Klaus B. Tenberge for his assistance with TEM, and Prof. Thierry Delair and Rémi Roux for their help with TF-IR measurements. This work was supported in part by the German Federal Ministry of Research and Education, BMBF.

References

Allan, G. G., & Peyron, M. (1995a). Molecular weight manipulation of chitosan I: Kinetics of depolymerization by nitrous acid. *Carbohydrate Research*, *277*, 257–272.

Allan, G. G., & Peyron, M. (1995b). Molecular weight manipulation of chitosan. II: Prediction and control of extent of depolymerization by nitrous acid. *Carbohydrate Research*, *277*, 273–282.

Bacon, W. C., Portyer, K. J., Noreed, P. W., & Leslie, F. J. (1996). Production of fusaric acid by Fusarium species. *Applied and Environmental Microbiology*, *62*, 4039–4043.

Benns, B. G., Gingras, B. A., & Bayley, C. H. (1960). Antifungal activity of some thiosemicarbazones and their copper complexes. *Applied Microbiology*, *8*, 353–356.

Borkow, G., & Gabbay, J. (2005). Copper as a biocidal tool. *Current Medicinal Chemistry*, *12*, 2163–2175.

Brunel, F., Veron, L., David, L., Domard, A., & Delair, T. (2008). A novel synthesis of chitosan nanoparticles in reverse emulsion. *Langmuir*, *24*, 11370–11377.

Brunel, F., Véron, L., Ladavière, C., David, L., Domard, A., & Delair, T. (2009). Synthesis and structural characterization of chitosan nanogels. *Langmuir*, *25*, 8935–8943.

Chiessi, E., Paradossi, G., Venanzi, M., & Pispisa, B. (1992). Copper complexes immobilized to chitosan. *Journal of Inorganic Biochemistry*, *46*, 109–118.

Deluisa, A., Giandon, P., Aichner, M., Bortolami, P., Bruna, L., Lupetti, A., et al. (1996). Copper pollution in Italian vineyard soils. *Communications in Soil Science and Plant Analysis*, *27*, 1532–2416.

Domard, A. (1987). pH and c.d measurements on a fully deacetylated chitosan: Application to Cu(II)-polymer interactions. *International Journal of Biological Macromolecules*, *9*, 98–104.

Hathaway, B., & Hodgson, P. (1973). Copper-ligand bond-lengths in axial complexes of the copper(II) ion. *Journal of Inorganic and Nuclear Chemistry*, *35*, 4071–4081.

Hirai, A., Odani, H., & Nakajima, A. (1991). Determination of degree of deacetylation of chitosan by ^{1}H NMR spectroscopy. *Polymer Bulletin*, *26*, 87–94.

Hoppe-Seiler, F. (1894). Über Chitin und Zellulose. *Berichte der Deutschen Chemischen Gesellschaft*, *27*, 3329–3331.

Ivanov, V. E., Tikhomirova, N. G., Tomchin, A. B., & Razukrantova, N. V. (1989). Antimicrobial and antibacterial activity of isatin thiosemicarbazones and their complex copper complexes (II) and (I). *Pharmaceutical Chemistry Journal*, *23*, 415.

Johna, R. P., Sreekantha, A., Rajakannanb, V., Ajithc, T., & Prathapachandra Kurup, M. (2004). New copper(II) complexes of 2-hydroxyacetophenone N(4)-substituted thiosemicarbazones and polypyridyl co-ligands: Structural, electrochemical and antimicrobial studies. *Polyhedron*, *23*, 2549–2559.

Kong, M., Chen, X. G., Xing, K., & Park, H. J. (2010). Antimicrobial properties of chitosan and mode of action: A state of the art review. *International Journal of Food Microbiology*, *144*, 51–63.

Koppel, D. E. (1972). Analysis of macromolecular polydispersity in intensity correlation spectroscopy: The method of cumulants. *Journal of Chemical Physics*, *57*, 4814–4820.

Lamarque, G., Viton, C., & Domard, A. (2004a). Comparative study of the first heterogeneous deacetylation of alpha- and beta-chitins in a multistep process. *Biomacromolecules*, *5*, 992–1001.

Lamarque, G., Viton, C., & Domard, A. (2004b). Comparative study of the second and third heterogeneous deacetylations of alpha- and beta-chitins in a multistep process. *Biomacromolecules*, *5*, 1899–1907.

Langmuir, I. (1918). The adsorption of gases on plane surfaces of glass, mica and platinum. *Journal of the American Chemical Society*, *40*, 1361–1368.

Langvad, F. (1999). A rapid and efficient method for growth measurement of filamentous fungi. *Journal of Microbiological Methods*, *37*, 97–100.

Lee, S. T., Mi, F. L., Shen, Y. J., & Shyu, S. S. (2001). Equilibrium and kinetic studies of copper(II) ion uptake by chitosan-tripolyphosphate chelating resin. *Polymer*, *42*, 1879–1892.

Luan, L. Q., Ha, V. T. T., Nagasawa, N., Kume, T., Yoshii, F., & Nakanishi, T. M. (2005). Biological effect of irradiated chitosan on plants in vitro. *Biotechnology and Applied Biochemistry*, *41*, 49–57.

Mekahlia, S., & Bouzid, B. (2009). Chitosan–copper (II) complex as antibacterial agent: Synthesis, characterization and coordinating bond-activity correlation study. *Physics Procedia*, *2*, 1045–1053.

Millardet, P. (1885). Sur l'histoire du traitement du mildiou par le sulphate de cuivre. *Journal d'Agriculture Pratique*, *2*, 801–805.

Moerschbacher, B. M., Bernard, F., & El Gueddari, N. E. (2011). Enzymatic/mass spectrometric fingerprinting of partially acetylated chitosans. *Advances in Chitin Sciences*, *13*, 185–191.

Monteiro, O. A. C., & Airoldi, C. (1999). Some thermodynamic data on copper–chitin and copper–chitosan biopolymer interactions. *Journal of Colloid and Interface Science*, *212*, 212–219.

Musinu, A., Paschina, G., Piccaluga, G., & Magini, M. (1983). Coordination of copper(II) in aqueous copper sulfate solution. *Inorganic Chemistry*, *22*, 1184–1187.

Muzzarelli, R. A. A. (1977). *Chitin*. Oxford, UK: Pergamon Press.

Muzzarelli, R. A. A. (2012). Nanochitins and nanochitosans, paving the way to eco-friendly and energy-saving exploitation of marine resources. In K. Matyjaszewski, & M. Möller (Eds.), *Polymer science: A comprehensive reference* (pp. 153–164). Amsterdam: Elsevier BV.

Ogawa, K., Oka, K., & Yui, T. (1993). X-ray study of chitosan–transition metal complexes. *Chemistry of Materials*, *5*, 726–728.

Oliveira, E., El Gueddari, N. E., Moerschbacher, B. M., Peter, M., & Franco, T. (2008). Growth of phytopathogenic fungi in the presence of partially acetylated chitooligosaccharides. *Mycopathologia*, *166*, 163–174.

Osman, Z., & Arof, A. K. (2003). FTIR studies of chitosan acetate based polymer electrolytes. *Electrochimica Acta*, *48*, 993–999.

Pontecorvo, G., Roper, J., Chemmons, L., Macdonald, K., & Bufton, A. (1953). The genetics of *Aspergillus nidulans*. *Advances in Genetics*, *5*, 141–238.

Prusky, D., & Yakoby, N. (2003). Pathogenic fungi: Leading or led by ambient pH? *Molecular Plant Pathology*, *4*, 509–516.

Qi, L., Xu, Z., Jiang, X., Li, Y., & Wang, M. (2005). Cytotoxic activities of chitosan nanoparticles and copper-loaded nanoparticles. *Bioorganic & Medicinal Chemistry Letters*, *15*, 1397–1399.

Rabea, E. I., Badawy, M. E. T., Stevens, C. V., Smagghe, G., & Steurbaut, W. (2003). Chitosan as antimicrobial agent: Applications and mode of action. *Biomacromolecules*, *4*, 1457–1465.

Rhazi, M., Desbrières, J., Tolaimate, A., Rinaudo, M., Vottero, P., & Alagui, A. (2002). Contribution to the study of the complexation of copper by chitosan and oligomers. *Polymer*, *43*, 1267–1276.

Rouget, C. (1859). Des substances amylacées dans le tissu des animaux, spécialement les Articulés (Chitine). *Comptes Rondus*, *48*, 792–795.

Smoluchowski, M. (1903). Essai d'une théorie cinétique du mouvement Brownien et des milieux troubles. *Bulletin International de l'Academie des Sciences de Cracovie*, *184*.

Swain, M. R., & Ray, R. C. (2009). Oxalic acid production by Fusarium oxysporum Schlecht and Botryodiplodia theobromae Pat. post-harvest fungal pathogens of yams (*Dioscorea rotundata* L.) and detoxification by Bacillus subtilis CM1 isolated from culturable cowdung microflora. *Archives of Phytopathology and Plant Protection*, *42*, 666–675.

Vachoud, L., Zydowicz, N., & Domard, A. (1997). Formation and characterisation of a physical chitin gel. *Carbohydrate Research*, *302*, 169–177.

Varma, A. J., Deshpande, S. V., & Kennedy, J. F. (2004). Metal complexation by chitosan and its derivatives: A review. *Carbohydrate Polymers*, *55*, 77–93.

Wan Ngah, W. S., Endud, C. S., & Mayanar, R. (2002). Removal of copper(II) ions from aqueous solution onto chitosan and cross-linked chitosan beads. *Reactive and Functional Polymers*, *50*, 181–190.

Wu, S. J., Liou, T. Z., Yeh, C. H., Mi, F. L., & Lin, T. K. (2012). Preparation and characterization of porous chitosan–tripolyphosphate beads for copper(II) ion adsorption. *Journal of Applied Polymer Science*, http://dx.doi.org/10.1002/APP.38073

Yan, H., Yang, L., Yang, Z., Yang, H., Li, A., & Cheng, R. (2012). Preparation of chitosan/poly (acrylic acid) magnetic composite microspheres and applications in the removal of copper(II) ions from aqueous solutions. *Journal of Hazardous Materials*, *229–230*, 371–380.

Zheng, Y., Yi, Y., Qi, Y., Wang, Y., Zhangb, W., & Du, M. (2006). Preparation of chitosan–copper complexes and their antitumor activity. *Bioorganic & Medicinal Chemistry Letters*, *16*, 4127–4129.